Dynamic Strength of the Interaction between Lung Surfactant Protein D (SP-D) and Saccharide Ligands†

Esben Thormann,[a*,‡] Jakob K. Dreyer,[§] Adam C. Simonsen,[‡] Per L. Hansen,[‡] Søren Hansen,[⊥] Uffe Holmskov,[∥] and Ole G. Mouritsen[‡]

MEMPHYS, Department of Physics and Chemistry, University of Southern Denmark, Campusvej 55, DK-5230 Odense M, Denmark, Respiratory Delivery Characterization, Novo Nordisk A/S, Brennum Park, DK-3400 Hillerød, Denmark, Medical Biotechnology Center, Institute of Medical Biology, University of Southern Denmark, Winsloewsparken 25,3, DK-5000 Odense C, Denmark, and Immunology and Microbiology, Institute of Medical Biology, University of Southern Denmark, Winsloewsparken 21,1 DK-5000 Odense C, Denmark

Received May 1, 2007; Revised Manuscript Received August 14, 2007

ABSTRACT: In order to investigate the dynamic strength of the interaction between lung surfactant protein D (SP-D) and different sugars, maltose, mannose, glucose, and galactose, we have used an atomic force microscope to monitor the interaction on a single molecule scale. The experiment is performed by measuring the rupture force when the SP-D−sugar bond is subjected to a continuously increasing force. Under these dynamic conditions, SP-D binds strongest to D-mannose and weakest to maltose and D-galactose. These results differ from equilibrium measurements wherein SP-D exhibits preference for maltose. On the basis of this finding, we propose that the binding of the disaccharide maltose to SP-D, which is energetically stronger than the binding of any of the monosacchrides, alters the structure of the binding site in a way that lowers the dynamic strength of the bond. We conclude that determining the strength of a protein−ligand bond under dynamic stress using an atomic force microscope is possibly more relevant for mimicking the actual nonequilibrium physiological situation in the lungs.

Surfactant protein D (SP-D[1]) belongs to a family of Ca^{2+}-dependent carbohydrate binding proteins designated collectins. SP-D is known to be an important part of the innate immune system and to modulate the adaptive immune system. This protein clears the lungs of bacteria, viruses, yeasts, and fungi by recognition of and selective binding to glycoconjugates on the surface of invading microorganisms (*1*−*3*). The majority of the proteins are found as dodecamers made of four identical trimeric subunits linked together via disulfide bonds in the N-termini. Each subunit is composed of three polypeptide chains characterized by an N-terminal region, a triple helical collagen-like region, a coiled-coil neck region, and the Ca^{2+}-dependent carbohydrate recognition domain. Carbohydrate binding takes place in the carbohydrate recognition domain, and in a number of experiments, the affinity for SP-D toward different carbohydrates has been tested in a competitive enzyme-linked immunosorbent assay (ELISA) (*4*−*6*). Here, the protein's ability to bind to a ligand-coated plastic surface, in competition with an unbound (different) ligand, is measured. These experiments have revealed that the binding energy of human SP-D to some common carbohydrates can be ordered as follows:

N-acetyl-mannosamine > Maltose > Glucose ≥ Mannose > Galactose > *N*-acetyl-glucosamine

such that SP-D has highest affinity for *N*-acetyl-mannosamine and lowest affinity for *N*-acetyl-glucosamine (see Table 1 for selected results). Comparison of the high-resolution X-ray structure of the carbohydrate recognition domain with and without bound maltose provides information about the nature of the bond between SP-D and a ligand (*7*, *8*). Even though maltose is a disaccharide, the first study (*7*) suggested that only the primary glucose units of maltose takes active part in bonding, while the secondary unit is either not taking part in the interaction or very loosely bound. However, more recent studies (*8*) show that the secondary and tertiary glucose units in maltotriose and in *p*-nitrophenyl-α-D-maltoside are also involved in the interaction. Furthermore, it is shown that the aromatic group in *p*-nitrophenyl-α-D-maltoside significantly enhances the interaction. The specific interaction itself is rather complex and involves the stabilization of a calcium ion in the binding site, hydrogen bonds, and van der Waals interactions. In addition, minor structural changes in the protein lead to enhanced intramolecular interactions. Thus, the strength of the interaction depends on the detailed molecular structure of the carbohydrate. For example, the direction of OH groups determines the ability

† This work was supported by the Danish National Research Foundation via a grant to MEMPHYS−Center for Biomembrane Physics (to E.T., A.C.S., P.L.H., and O.G.M.), the NKT-academy (to J.K.D.). and the Danish Medical Research Council (S.H.).

* Corresponding author. Tel: +45 6550 3474. Fax: +45 6550 4048. E-mail: esbent@memphys.sdu.dk.

‡ MEMPHYS, University of Southern Denmark.

§ Novo Nordisk A/S.

∥ Medical Biotechnology Center, University of Southern Denmark.

⊥ Immunology and Microbiology, University of Southern Denmark.

[1] Abbreviations: AFM, atomic force microscope; BSA, bovine serum albumin; ELISA, enzyme-linked immunosorbent assay; PBS, phosphate buffered saline; PEG, poly(ethylene glycol); SDS−PAGE, sodium dodecyl sulfate polyacrylamide gel electrophoresis; SMB, succinimidyl α-methylbutanoate; SP-D, surfactant protein D; Tris, tris(hydroxymethyl)methylamine.

10.1021/bi700823k CCC: $37.00
Published on Web 10/04/2007

Table 1: Most Likely Unbinding Force, F^*, for the SP-D−Carbohydrate Systems Defined As the Peak Bin-Values in the Histograms and the Position of the Maximum of a Gaussian Fit to the Histograms[a]

ligand	F^* (histogram)	F^* (Gaussian fit)	I_{50} (mM)
maltose	40 ± 2.5 pN	43 ± 3.9 pN	2.7
mannose	55 ± 2.5 pN	54 ± 1.7 pN	5.3
glucose	45 ± 2.5 pN	47 ± 2.3 pN	4.1
galactose	35 ± 2.5 pN	38 ± 2.0 pN	10

of the monosaccharide to form hydrogen bonds with SP-D. The strength of the interaction is determining the affinity of SP-D for carbohydrates found on microbial surfaces and is thus important for SP-D's function in the immune system.

Saccharide preference was measured by ELISA and hence relative estimates of affinities are thermodynamic quantities where the amount of SP-D bound to a certain ligand is determined by the lowest free energy state. One *in vivo* function of SP-D is to bind and cross-link pathogens that are invading the lungs. During breathing with resulting lung inflation and deflation, a significant liquid flow will take place in the alveolar hypophase. This is because the thickness of this aqueous layer will decreases during lung inflation and increases again during lung deflation. Since the size of invading pathogens is comparable with the thickness of the aqueous layer, some sticking to the boundaries is likely to occur. Because of the liquid flow, a molecular complex of cross-linked pathogens will thus be subjected to a high degree of mechanical stress. Therefore, the binding and unbinding of SP-D to carbohydrates on the surface of the microorganisms will in general not take place under static thermal conditions. A similar conclusion can be drawn for molecular complexes of SP-D in the upper airways and respiratory tract where mucociliary transportation is the source of mechanical stress.

Therefore, we have studied the stability of a single SP-D−sugar bond under conditions where it is subjected to dynamic mechanical stress. An atomic force microscope (AFM) has been used to investigate the interaction between SP-D and carbohydrates on a single molecule scale. During the past decade, dynamic force spectroscopy performed with AFM has proven to be a powerful tool for the investigation of single molecule interaction and mechanics (*9*−*13*). Experiments for the investigation of protein−ligand interactions can be performed by anchoring the protein to a surface and the ligand to the tip of an AFM cantilever or vice versa. When the tip is directed toward the surface, a binding event between a single protein and a ligand can take place. Subsequently, when the tip is gradually retracted from the surface, a continuously increasing force is applied to the bond until it eventually breaks (see Figure 1). Breaking a molecular bond is a kinetic phenomenon that is fundamentally caused by the thermal energy in the system. At any time interval, there is always a nonzero probability of rupturing. Thus, the unbinding between two molecules induced by an applied force in an AFM experiment is a stochastic process where the average unbinding force will depend on the nature of the bond as well as how the mechanical stress is applied (*11*, *14*). The average force needed to break a bond between a protein and a ligand is not necessarily related to the equilibrium stability of the bond but is rather a measure of

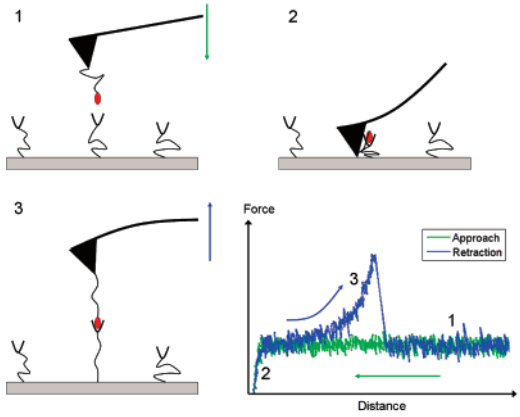

FIGURE 1: Illustration of the steps in a single molecule AFM experiment and a so-called force curve where the force between the AFM-tip and the surface is plotted vs the tip−surface separation. In step 1, the tip is approaching the surface, and no force is detected (green curve). In step 2, the tip comes into contact with the surface, which gives rise to a strongly repulsive force. In step 3, the cantilever is retracted from the surface, and because of the binding event between two molecules bridging the tip and the surface, an attractive force is now observed (blue curve).

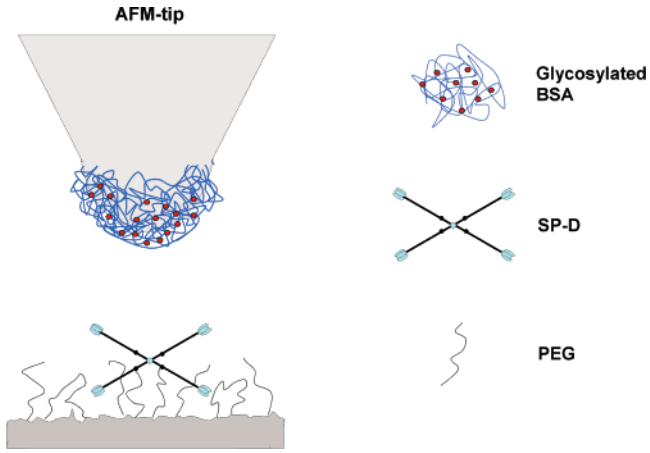

FIGURE 2: Illustration of the functionalized AFM-tip and surface. SP-D is anchored to the surface by a PEG-linker, and glycosylated BSA is adsorbed onto the AFM-tip.

the dynamic strength when mechanical stress is applied to the system. In this article, we have used this technique to investigate the dynamic strength of the interaction between SP-D and each of the three monosaccharides, mannose, glucose, and galactose, as well as the disaccharide, maltose.

EXPERIMENTAL PROCEDURES

Experiments are performed by attachment of SP-D to a glass surface via a poly(ethylene glycol) (PEG) linker, and the carbohydrate ligands are attached to the AFM tip by the adsorption of glycosylated bovine serum albumin (BSA) (see Figure 2). Before use, both the substrate and the AFM cantilevers were ultrasonicated in water and ethanol followed by radio frequency-generated plasma treatment.

Purification of SP-D. SP-D was purified from human amniotic fluid by the principles described by Strong and coworkers (*15*). Briefly, amniotic fluid was centrifuged (800*g*, 4 °C, 20 min) to remove cells and loaded on to a column made of maltose−agarose (Sigma, Denmark) in the presence of Ca^{2+}. After washing with Ca^{2+} containing buffers, SP-D was eluted with a Mn^{2+} containing buffer. Furthermore,

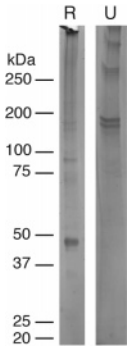

FIGURE 3: Purified SP-D. SP-D was purified from human amniotic fluid by combinatorial maltose affinity and ion exchange chromatography. The final eluate was analyzed by SDS−PAGE on a 4−12% gradient gel. R, reduced and alkylated; U, unreduced. The estimated molecular weights correspond to the mobility of the used globular marker proteins.

purification was achieved by ion-exchange chromatography using a Mono-Q column (Amersham, Pisctatway, NJ) at pH 8.3 and elution by a 50−750 mM gradient of NaCl. As judged by means of SDS−PAGE and silver staining, the final SP-D preparation was more than 95% pure (see Figure 3). The relative content of dodecamers versus single subunits made of three polypeptide chains was, as judged by gel permeation chromatography, 70% versus 30% in favor of dodecameric SP-D. The oligomerization varied (± 15%) from batch to batch. Estimation of the concentration of SP-D was done by means of ELISA as previously described (*16*).

Surface Functionalization. A clean microscope cover glass (Menzel-gläser) was first incubated in a 2.0% solution of aminopropyltrietoxysilane in dry toluene for 2 h followed by rinsing with toluene, toluene/ethanol (1:1), and ethanol. Thereafter, the glass slide was incubated in an oven at 150 °C for 15 min. This step leaves the surface covered by NH_2 groups. The substrate was now incubated in a 5 mM solution of SMB-PEG-SMB ($M_W \approx 3400$ g/mol, Shearwater Polymer) in DMSO for 3 h, followed by rinsing in DMSO, and dried under low pressure. In this step, the SMB (succinimidyl α-methylbutanoate) groups on the PEGs bind covalently to the amino groups on the surface. Because of the symmetry of the functionalized groups on the polymer, some of the polymers are expected to be attached with both ends to the surface. However, by using high polymer concentration, a considerable fraction of the polymers are expected to be attached to the surface by only one of the ends. The attachment of human SP-D was facilitated by incubating the PEG-functionalized cover glass in a 30 μg/mL solution of SP-D in phosphate buffered saline (PBS) at pH 8.25 for 2 h. In this step, the SMB on the free end of the PEG binds covalently to lysine on the SP-D. The pH was adjusted to 8.25 to increase the rate of SP-D−SMB binding, which is in competition with SMB hydrolysis. Under these conditions, the hydrolytic half-life time of the SMB-PEG-SMB is 44 min. Finally, the glass slide was moved to a container with Tris/$CaCl_2$ buffer (145 mM NaCl, 10 mM Tris, and 3 mM $CaCl_2$ at pH 7.4) to both stabilize the protein and to activate the binding site.

Tip Functionalization. Attachment of the carbohydrate to the tip was accomplished by incubating the cantilever in a 1 mg/mL solution of glycosylated BSA (bovine-maltosyl albumin, bovine α-D-manno pyranosylphenyl albumin, bovine-glucosamide albumin, or bovine-galactosamide albumin, all purchased from Sigma, Denmark) in PBS (pH 7.4) over night. BSA binds strongly by nonspecific adsorption to the AFM tip, and additional BSA was removed by flushing the cantilever with Tris/$CaCl_2$ buffer (pH 7.4) before use. The density of sugar groups on the AFM tip will vary between experiments because of different levels of saccharide substitution and because the exact amount of glycosylated BSA adsorbed during incubation will differ. While this will influence the binding frequency, it will not influence the force needed to break the bond between SP-D and a single ligand.

Force Measurements. Force measurements were carried out on a JPK NanoWizard (JPK Instruments, Berlin, Germany) in a commercial liquid cell from JPK Instruments containing Tris/$CaCl_2$ buffer (pH 7.4). Rectangular cantilevers (MSCT-AUHW B-lever, Veeco) were used, and the spring constant was determined by both the Hutter and Bechhoefer method (*17*) and by the Sader method (*18*). As previously shown, the relationship between cantilever stiffness and molecular compliance influences the outcome of an experiment in a complex way (*11*). To simplify matters, four cantilevers with very similar spring constants were used. The spring constants were determined to be 20.8, 21.0, 21.1, and 21.5 pN/nm, respectively. All force curves were recorded at a constant approach and retraction velocity of 500 nm/s.

RESULTS

When the AFM tip covered by glycosylated BSA is moved toward the surface, a sugar molecule can be bound to any of the 12 binding sites on an SP-D dodecamer. Upon the subsequent retraction of the cantilever, the polymer that anchors SP-D to the surface will be stretched out because of the continuously increasing force on the bond. Taking into account the length of the polymer linker (30 nm) and the length of SP-D (100 nm) (*18*), the bond is expected to break at a surface−tip separation of approximately 30−130 nm, depending on the orientation of SP-D and the SP-D binding site that is involved. Examples of retraction force curves showing unbinding events between SP-D and mannose are shown in Figure 4A. The molecules unbind within the expected range of surface−tip separations, and the unbinding force varies from 40−100 pN, which is within the range of unbinding forces measured for other collectin−carbohydrate systems (*20*, *21*). A variation in the unbinding force is expected because of the stochastic nature of the process, and hundreds of unbinding events therefore need to be recorded in order to obtain reliable statistics.

Here, we have investigated the interaction between SP-D and maltose, mannose, glucose, and galactose, and the data have been analyzed as described above. In Figure 5, histograms of unbinding forces from experiments with the four different sugars are shown. The magnitude of the most likely unbinding forces, F^*, is determined both as the maximum bin values and by Gaussian fits to the histograms; the values are given in Table 1. The results show that there is a significant difference in the typical force needed to break the bond between SP-D and each of the sugar molecules. This dynamical binding strength between SP-D and different sugars can be ordered as follows:

mannose > glucose > maltose > galactose

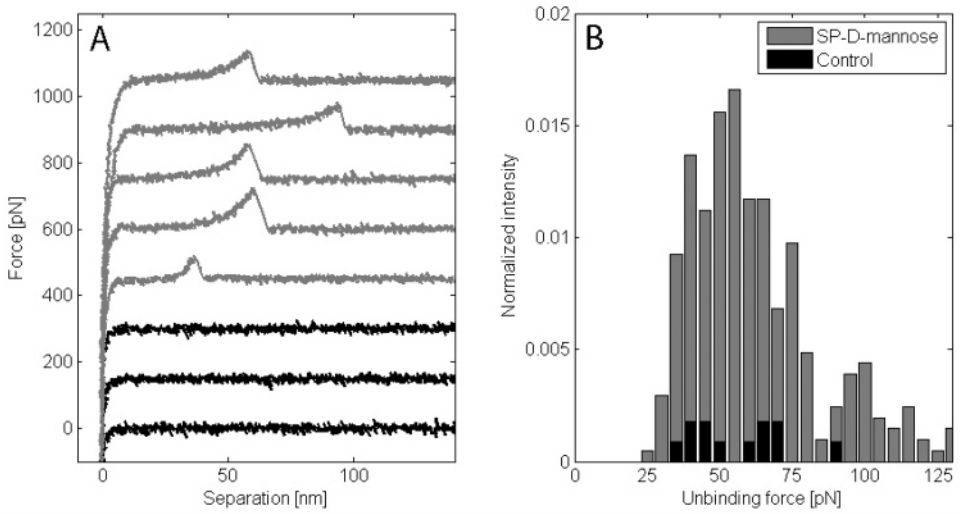

FIGURE 4: (A) Gray curves are typical retraction force curves obtained with SP-D anchored to the surface and mannose-BSA adsorbed to the AFM-tip. The unbinding distance differs depending on where the polymer linker is attached to SP-D and which carbohydrate recognition domains is reached by the incoming saccharide ligand. The shape of the force curves prior to unbinding reflects the elastic response of the linker molecules and of SP-D. Black curves are typical retraction force curves for the same system obtained after the addition of 50 mM free maltose. These force curves show no interaction between the ligand coated AFM-tip and the SP-D coated surface, which is similar to the interaction expected for an uncoated AFM-tip. The zero-point of the force is in these force curves offset to make the individual curves distinguishable. (B) Histograms of unbinding force before (gray) and after (black) the addition of free maltose. The number of binding events is normalized by the number of approach/retraction cycles.

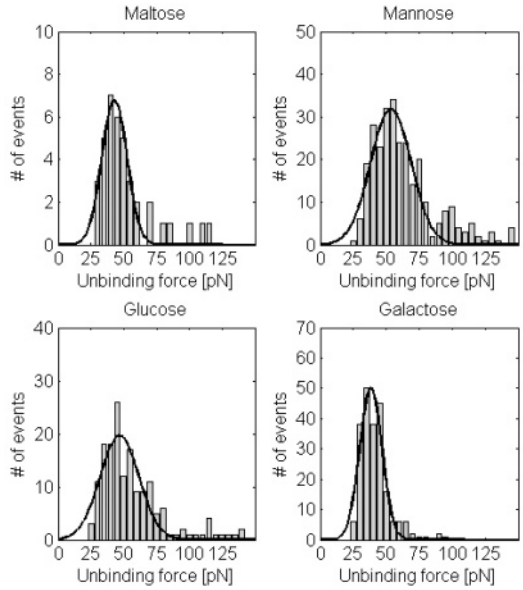

FIGURE 5: Histograms of unbinding forces for the interaction between SP-D and maltose, mannose, glucose, and galactose, respectively. Gaussian functions are fitted to the distributions with a cutoff at 85 pN. The values of the most likely unbinding forces are reported in Table 1.

where mannose has the highest unbinding force, and maltose and galactose have the lowest unbinding force of the four tested sugars.

Control for Specificity. A crucial aspect of the studies of single molecular interaction is to verify that the observed unbinding events are actually due to specific interaction between the protein and the ligand and not due to some kind of nonspecific interaction. We have carried out tests to verify the specificity of the interaction. First, the surface−tip separation where the unbinding takes place fits well with the combined length of the polymer linker and the size of the protein. Nonspecific binding due to, for example, adhesion of BSA to the surface or polymer−BSA entanglement is also observed in this study. However, these events lead to significantly higher unbinding forces and unbinding events that always takes place at surface−tip separations below 20 nm. Second, the fact that different unbinding forces are observed for the four different sugars used in this study is an important indication of the specificity of the interaction. The disparity between the effects of the different ligands cannot be an artifact due to sample preparation since repeated experiments confirm the results presented in Table 1 within confidence intervals (data not shown). The final test of specificity of the interaction is to block the binding site in SP-D with a free ligand. An experiment with SP-D anchored to the surface and mannose-BSA adsorbed on the AFM tip was conducted. Data from 2050 approach and retraction cycles were initially collected, and 11.5% of the retraction force curves showed unbinding events at tip−surface separations of 30−130 nm and were thus expected to be due to specific binding. After the first 2050 force curves, the Tris/$CaCl_2$ buffer was exchanged with a Tris/$CaCl_2$ buffer containing 50 mM free maltose. Thereafter, additional 1127 force curves were collected and analyzed in the same way. After the addition of free maltose, specific binding events were observed in less than 1% of the retraction force curves in accordance with the fact that most binding sites are blocked by the free ligand (see Figure 4B). The last question is whether we are actually measuring the rupture of single bonds or whether multiple binding occurs. The size of the protein (100 nm) compared to the radius of curvature of the AFM tip (<50 nm) makes interaction between the tip and more than a single protein unlikely. However, since one SP-D dodecamer has 12 binding sites, multiple binding to one protein could occur. To investigate this further, we have performed a series of blocking experiments similar to the experiment described in relation to Figure 4. To block or inhibit multiple binding, we have used relatively low concentrations of free maltose, which only causes a partial blocking of the binding sites on SP-D. A partial blocking

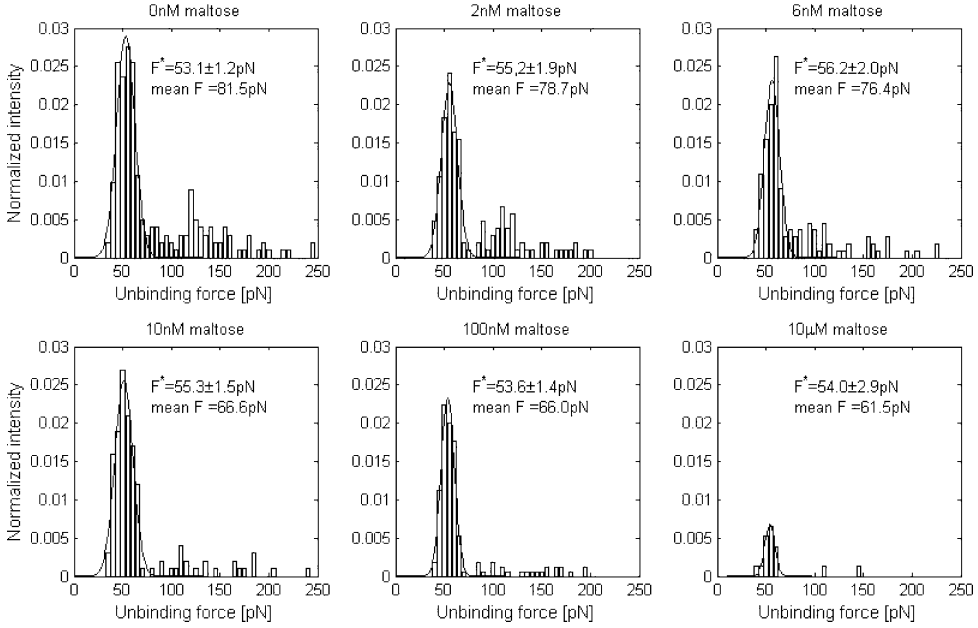

FIGURE 6: Histograms of unbinding forces between SP-D and mannose in buffer containing free maltose. A low concentration of free maltose leads to a partial blocking of the binding site on SP-D. This partial blocking decreases the probability of binding between SP-D and mannose attached to the AFM-tip, and in particular, it decreases the probability for multiple binding events. Besides the main population of unbinding events, with a maximum around 55 pN, additional populations with unbinding forces of more than 70 pN are also observed in the complete absence or in the presence of low concentrations of free maltose (<10 nM). The population around 55 pN is ascribed to unbinding events between SP-D and a single ligand, while unbinding events at higher forces are ascribed to multiple binding. As the concentration of free maltose is decreased, the unbinding event at higher forces vanishes, and the overall binding frequency decreases. However, the maximum of the population ascribed to unbinding events between SP-D and a single ligand remain unchanged, which substantiates this assumption.

will lower the binding frequency and thereby the likelihood of multiple binding. The result of this experiment is shown in Figure 6. Inhibiting with 0−10 nM free maltose results in a main population of unbinding events with a maximum around 55 pN. A less prominent population at around 100−150 pN is also observed and indicates that some degree of multiple binding does occur. As the concentration of free maltose increases, the mean unbinding force gradually decreases because multiple binding becomes less likely. However, while the mean unbinding force decreases, the maximum of the main population is unchanged. This clearly shows that the main population corresponds to rupture events between SP-D and a single ligand. As the concentration of free maltose is increased even further, multiple binding becomes rare, but as most binding sites are blocked, the binding frequency is also significantly lowered. If the main population of unbinding forces corresponded to multiple unbinding events, for example, with multiple binding within one trimer of SP-D, a shift in the distribution of unbinding forces toward lower forces would be expected. Such low forces could easily be detected by the current experimental setup. All these tests make us confident that we are indeed measuring the specific interaction between a single SP-D and a single saccharide ligand.

DISCUSSION

We have measured the single-molecule interaction between SP-D and maltose, mannose, glucose and galactose. The results reveal that the SP-D−mannose bond can withstand the highest force, while the SP-D−maltose and SP-D−galactose bonds appear to be the weakest. These results partly deviate from ELISA data (*4*, *5*), which show that maltose has the highest affinity for SP-D, while in the present study, it could withstand lower force than mannose and glucose. Recent studies have revealed that it is not straightforward to correlate the affinity of the free sugars with more complex sugars (*8*). Interactions with immobilized monosaccharides conjugated to a protein carrier may take advantage of interactions between the linker molecule and amino acid residues located outside the binding site (*8*). In addition, interactions with complex sugars and microbial surfaces may also require a certain degree of flexibility and stretching to separate ligand-binding sites to a given pattern on the complex ligand (*22*). Both scenarios of interactions will not be assessed using unconjugated free sugars as inhibitors of binding. However, in this case, the critical factor is that the dynamic stability of a single molecular bond gives a different type of information than a measurement performed under equilibrium conditions. The amount of SP-D bound to a ligand under equilibrium conditions is given by the lowest free energy state and is therefore related to the ratio between the on-rate and off-rate, expressed by the equilibrium constant, $K = k_{on}/k_{off}$. The force needed to break an SP-D−sugar bond is related to the force-induced off-rate, $k_{off}(F)$ that is again related to the thermal off-rate, the shape of the energy landscape along the unbinding pathway as well as the dynamic stress history (e.g., the retraction velocity). Following Kramer's theory for diffusion over a single sharp barrier (*14*, *23*−*26*), the force-induced off-rate is approximately given by

$$k_{off}(F) = A \exp\left(-\frac{\Delta E_a - F(t)x_b}{k_B T}\right)$$

$$= k_{\text{off}} \exp\left(\frac{Fx_b}{k_B T}\right) \quad (1)$$

and the most likely unbinding force, F^*, by

$$F^* = \frac{k_B T}{x_b} \ln\left(\frac{k_s v x_b}{k_{\text{off}} k_B T}\right) \quad (2)$$

where A is known as the Arrhenius prefactor, ΔE_a is the height of the energy barrier, F is the applied force, x_b is a parameter giving the position of the barrier relative to the potential minimum, k_B is Boltzmann's constant, T is the temperature, k_s is proportional to the total elastic response of the AFM cantilever and the molecules bridging the AFM tip and the surface (*11*), and v is the retraction velocity of the cantilever. Within the framework of this simple model, it can be shown that the thermal off-rate and thereby the equilibrium stability are primarily related to the height of the energy barrier, while the force-induced off-rate and thereby the most likely unbinding force are dependent both on the height of the barrier and the position of the barrier. The fact that these two fundamentally different experiments provide different results is therefore not unexpected. In reality, the SP-D−sugar interaction is likely to be more complex than that described by a simple potential function, but the model will nonetheless show the essential behavior.

Two mechanisms are responsible for the strong interaction between a protein and a ligand. First, the ligand has to fit into the binding site and take part in intermolecular interactions, such as electrostatic interaction, hydrogen bonds, hydrophobic interactions, and so forth (the lock and key mechanism). Second, the protein can make minor structural transitions to enhance the interaction (induced fit). From X-ray studies, there is no doubt that both mechanisms are important for the SP-D−sugar interaction (*7*, *8*). If we consider the three monosaccharides, mannose, glucose, and galactose, they are all aldohexoses and thus stereoisomers of the same molecule. With respect to the size of the carbon backbone of the aldohexoses, this fit equally well into the binding site, but the isomerism of the hydroxyl groups provides them with a different ability to form hydrogen bonds with SP-D. This is the reason why mannose has a stronger interaction with SP-D than galactose, why SP-D has a high equilibrium affinity for mannose, and why the SP-D−mannose bond has a high dynamic strength. Maltose apparently does not fit into this picture, and an alternative explanation is called for. Within the framework of the simple model introduced above, two molecular bonds that have similar equilibrium stability can have a different dynamic stability if the position of the energy barrier in the interaction potential is different in the two cases. This situation, which is sketched in Figure 7, can serve as the simplest possible explanation of the results presented here. It is known that the second glucose unit in maltose takes part in the interaction and that this slightly changes the structural rearrangement of the binding site compared to that when SP-D is binding to glucose. Although, the structural changes of the binding site are subtle, they might, when shear stress is applied, shift the energy landscape and energy barrier toward an unfavorable situation. This may explain why maltose is not the most potent ligand in our studies. Unlike the previous ELISA-based estimations of ligand preferences, our current setup uses immobilized SP-D and immobilized sugar ligands. We cannot exclude that this might have an effect on our observations and even the physiological relevance hereof. However, *in vivo* ligands for SP-D are not normally free in solution but rather are part of a complex microbial surface. As SP-D binds to both the phoshoinositol phosphate in the surfactant and to alveolar macrophages, it is unlikely that SP-D itself is "free" in solution. Thus, we expect that the current setup is a representative model for the shear forces applied to SP-D's interactions. We again acknowledge that the SP-D−sugar interaction is much more complex than the interaction potentials presented in Figure 7, but this can serve as a minimal model to rationalize the observed trends. Additionally, it should be stressed that the unbinding force also depends on the so-called loading rate, $r = vk_s$ (see eq 4). This means that the order of the dynamic strength observed in this study could possibly change if a different loading rate is used. However, a retraction velocity, $v = 500$ nm/s, gives a loading rate that is comparable with the loading rate used in previous protein−ligand studies. Furthermore, the effective loading rate, $r \approx 100$ pN/s, calculated from the linker stiffness just prior to bond failure, is comparable to an estimated value of the effective loading rate, and the bond will be subjected to thermal fluctuations of abacterial membrane. Thus, we believe this a good starting point for a discussion of dynamic versus equilibrium stability of molecular bonds.

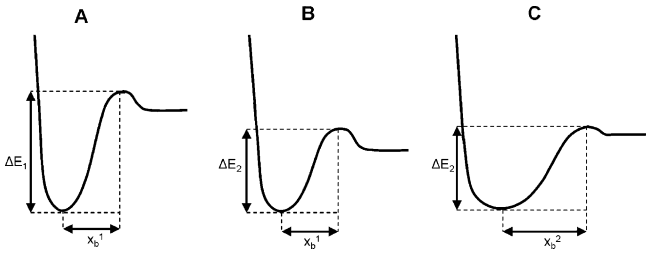

FIGURE 7: Illustration of three simple interaction potentials that qualitatively explains the difference between equilibrium and dynamic stability.Potentials A and B have the barriers located at the same distance from the energy minimum, but the potential well is deeper in A than in B. The difference between A and B implies that A will lead to a stronger interaction than B, both with respect to equilibrium stability and dynamic stability. A and B can therefore qualitatively rationalize the difference between the SP-D−mannose interaction (A) and the SP-D−galactose interaction (B). Potentials B and C have the same depth, but the barriers are located at different distances from the energy minimum. The difference between B and C implies that both systems will have a similar equilibrium stability but a very different dynamic stability. Since the barrier in C is located further away from the energy minimum, this system will be more sensitive to an applied force and therefore have a lower dynamic stability. B and C can therefore qualitatively rationalize the observed experimental difference between the SP-D−glucose interaction (B) and the SP-D−maltose interaction (C).

Finally, it should also be mentioned that in the particular case of selectin−ligand bonds (*27*, *28*) it was found that an applied force can change the molecular structure of selectin and thereby enhance the strength of the bond, the so-called catch bonds phenomenon. Under physiological conditions, the interactions between leukocyte selectins with molecules on the endothelium are prone to shear stress. The applied force from the shear stress originates from the hydrodynamic forces of blood flow and leads to a decreased number of unbinding events and hence increased adhesion to the

endothelium. Although SP-D's physiological interactions with both microbial ligands and lung surfactant are not prone to shear forces from an unidirectional blood flow, they are prone to other shear stresses. The shear stress originates from the continual deflation and inflation that relaxes and stretches the epithelium, respectively, and requires the redistribution of the surfactant covering the epithelium. In the upper airways, aggregates of SP-D and microorganisms experience shear stress because of the mucociliary transportation. On the basis of the current work, we hypothesize that the catch bond phenomenon also applies to SP-D's interactions and that it is optimized to serve SP-D functions in both phospholipid homeostasis and clearance of microorganisms. In any case, the unbinding pathway might be dependent on the applied force, a feature that is not accounted for by simple interaction potentials as shown in Figure 7.

To our knowledge, the SP-D−sugar system is the first where an apparent discrepancy between the dynamic stability of a molecular bond and the thermodynamic stability of the same molecular complex has been observed. This finding could be of significant importance for the protein function *in vivo*, where molecular interactions typically do not take place under equilibrium conditions. The results indicate that the stability of biomolecular complexes depends on the way it is measured and that the stability should be measured by a technique that matches the physiological conditions. Specifically, this work suggests the importance of the use of AFM studies of other biomolecular interactions where dynamic properties are expected.

REFERENCES

1. Wright, J. R. (2005) Immunoregulatory functions of surfactant proteins, *Nature Rev. Immunol. 5*, 58−68.
2. Kingma, P. S., and Whitsett, J. A. (2006) In defence of the lung: surfactant protein A and surfactant protein D, *Curr. Opin. Pharmacol. 6*, 277−283.
3. Hansen, S., Lo, B., Evans, K., Neophytou, P., Holmskov, U., and Wright, JR. (2007) Surfactant protein D augments bacterial association but attenuates major histocompatibility complex class II presentation of bacterial antigens, *Am. J. Respir. Cell. Mol. Biol. 36*, 94−102.
4. Persson, A., Chang, D., and Crouch, E. (1990) Surfactant protein D is a divalent cation-dependent carbohydrate binding protein, *J. Biol. Chem. 265*, 5755−5760.
5. Lu, J., Willis, A. C., and Ried, K. B. M. (1992) Purification, characterization and cDNA cloning of human lung surfactant protein D, *Biochem. J. 284*, 795−802.
6. Crouch, E. C, Smith, K., McDonald, B., Briner, D., Linders, B., Mcdonald, J., Holmskov, U., Head, J., and Hartshorn, K. (2006) Species differences in the carbohydrate binding preferences of surfactant protein D, *Am. J. Respir. Cell Mol. Biol. 35*, 84−94.
7. Shrive, A. K., Tharia, H. A., Strong, P., Kishore, U., Burns, I., Rizkallah, P. J., Reid, K. B. M., and Greenhough, T. J. (2003) High-resolution structural insights into ligand binding and immune cell recognition by human lung surfactant protein D, *J. Mol. Biol. 331*, 509−523.
8. Crouch, E., McDonald, B., Smith, K., Cafarella, T., Seaton, B., and Head, J. (2006) Contributions of phenylalanine 335 to ligand recognition by human surfactant protein D, *J. Biol. Chem. 281*, 18008−18014.
9. Lee, C.-K., Wang, Y.-M., Huang, L.-S., and Lin, S. (2007) Atomic force microscopy: Determination of unbinding force, off rate and energy barrier for protein-ligand interaction, *Micron 38*, 446−461.
10. Thormann, E., Evans, D. R., and Craig, V. S. J. (2006) Experimental studies of the dynamic mechanical response of a single polymer chain, *Macromolecules 39*, 6180−6185.
11. Thormann, E., Hansen, P. L., Simonsen, A. C., and Mouritsen, O. G. (2006) Dynamic force spectroscopy on soft molecular systems: Improved analysis of unbinding spectra with varying linker compliance, *Colloid Surf., B 53*, 149−156.
12. Strunz, T., Oroszlan, K., Schäfer, R., and Güntherodt, H.-J. (1999) Dynamic force spectroscopy of single DNA molecules, *Proc. Natl. Acad. Sci. U.S.A. 96*, 11277−11282.
13. Grandbois, M., Beyer, M., Rief, M., Clausen-Schaumann, H., and Gaub, H. E. (1999) How strong is a covalent bond? *Science 283*, 1727−1730.
14. Evans, E., and Ritchie, K. (1997) Dynamic strength of molecular adhesion bonds, *Biophys. J. 72*, 1541−1555.
15. Strong, P., Kishore, U., Morgan, C., Lopez, Bernal, A., Singh, M., and Reid, K. B. (1998) A novel method of purifying lung surfactant proteins A and D from the lung lavage of alveolar proteinosis patients and from pooled amniotic fluid, *J. Immunol. Methods 220*, 139−149.
16. Leth-Larsen, R., Nordenbaek, C., Tornoe, I., Moeller, V., Schlosser, A., Koch, C., Teisner, B., Junker, P., and Holmskov, U. (2003) Surfactant protein D (SP-D) serum levels in patients with community-acquired pneumonia, *Clin. Immunol. 108*, 29−37.
17. Hutter, J. L., and Bechhoefer, J. (1993) Calibration of atomic-force tips, *Rev. Sci. Instrum. 64*, 1868−1873.
18. Sader, J. E., Chon, J. W. M., and Mulvaney, P. (1999) Calibration of rectangular atomic force microscope cantilevers, *Rev. Sci. Instrum. 70*, 3967−3969.
19. Crouch, E. C. (1998) Structure, biologic properties, and expression of surfactant protein D (SP-D), *Biochim. Biophys. Acta 1408*, 278−289.
20. Touhami, A., Hoffmann, B., Vasella, A., Denis, F. A., and Dufrene, Y. F. (2006) Probing specific lectin-carbohydrate interactions using atomic force microscopy imaging and force measurements, *Langmuir 19*, 1745−1751.
21. Zhang, X., Bogorin, D. F., and Moy, V. T. (2004) Molecular basis of the dynamic strength of the sialyl lewis x−selectin interaction, *ChemPhysChem 5*, 175−182.
22. Dong, M., Xu, S., Oliveira, C. L., Pedersen, J. S., Thiel, S., Besenbacher, F., and Vorup-Jensen, T. (2007) Conformational changes in mannan-binding lectin bound to ligand surfaces, *J. Immunol. 178*, 3016−3022.
23. Kramers, H. A. (1940) Brownian motion in a field of force and the diffusion model of chemical reactions, *Physica (Utrecht) 7*, 284−304.
24. Hänggi, P., Talkner, P., and Borkovec, M. (1990) Reaction-rate theory: 50 years after Kramers, *Rev. Mod. Phys. 62*, 251−341.
25. Evans, E. (1998) Energy landscapes of biomolecular adhesion and receptor anchoring at interfaces explored with dynamic force spectroscopy, *Faraday Discuss. 111*, 1−16.
26. Dreyer, J. K., Berg-Sørensen, K., and Oddershede, L. (2006) Quantitative approach to small-scale nonequilibrium systems, *Phys. Rev. E 73*, 051110.
27. Marshall, B. T., Long, M., Piper, J. W., Yago, T., McEver, R. P., and Zhu, C. (2003) Direct observation of catch bonds involving cell-adhesion molecules, *Nature 423*, 190−193.
28. Evans, E., Leung, A., Heinrich, V., and Zhu, C. (2004) Mechanical switching and coupling between two dissociation pathways in a P-selectin adhesion bond, *Proc. Natl. Acad. Sci. U.S.A. 101*, 11281−11286.
29. *a*The uncertainties in the two cases are given by half of the bin size and as a 95% confidence interval for the mean of a normal distribution. I_{50} values were adapted from ref *6*.

BI700823K